43rd AIAA/ASME/ASCE/AHS/ASC Structures, Structural Dynamics, and Materials Con
22-25 April 2002, Denver, Colorado

AIAA-2002-1347

Computational Modeling of Damage Growth in Composite Laminates

Shiladitya Basu, Anthony M. Waas and Damodar R. Ambur [1]

March 31,2002
Composite Structures Laboratory
Department of Aerospace Engineering
University of Michigan, Ann Arbor, MI, 48109-2140

Abstract

A progressive damage growth model is developed for composite laminates under compression. The mechanics of damage initiation and growth in a single lamina is modeled in a 2D plane stress setting, using a system of orthotropic nonlinear elastic relations and a set of Internal State Variables. The latter are associated with different damage mechanisms that are unique to a fiber reinforced lamina. A thermodynamically consistent set of equations are formulated for the evolution of damage growth. The formulation is numerically implemented using the commercially available finite element package, ABAQUS. The present method is applied to analyze the problem of damage growth in a compressively loaded notched laminate. Predictions of the model compared against available experimental data are promising.

[1] Graduate Research Assistant, Professor of Aerospace Engineering, University of Michigan, and, Head, Mechanics and Durability Branch, NASA Langley Research Center, Hampton, VA, respectively.

1 Introduction

Development of computational methodologies for the prediction of progressive damage growth in continuous fiber composite laminates is presently an active area of research. Available predictive methods are based on defining strength based criteria at the lamina level. Based on critical values for tensile, compressive and shear 'strengths', these methods compute pre-defined damage indices that are expressed in functional form in terms of the current stress state. When any of these indices exceeds a predefined critical value, the material is said to have failed [1]. Beyond initial failure, a consistent and rigorous methodology to account for progressive material deterioration has not been investigated thoroughly. An exception to this is the work by Schapery and co-workers[2], who carried out lamina level tests, and validated the test results by developing a thermodynamically based progressive damage formation and growth model. In these studies, Schapery and co-workers assumed that the fiber direction response is essentially linear (slight elastic nonlinearity in the fiber direction was accounted for), but, damage (microcracking and transverse cracking) formation affect the response in the transverse direction. Consequently, internal state variables that are related to the damage mechanisms in the transverse direction were identified and evolution laws that specify the growth of damage and hence its influence on the transverse direction response were prescribed. In the present paper, Schapery's theory (ST) is extended to account for fiber direction damage (both, in tension and compression) by identifying an additional internal state variable associated with the fiber direction response. In contrast to the transverse direction, in which damage accumulation results in progressively decreasing but smooth variations in instantaneous tangent moduli, damage accumulation in the fiber direction leads to non-smooth abrupt changes in the corresponding moduli. These changes must be properly captured if progressive damage growth in composite laminates is to be modeled accurately. In the present paper, we have shown, for the first time, that it is possible to follow the progression of damage beyond first kinking in compressively loaded compos-

ite laminates using the Extended Schapery Theory (EST).

Tests in the fiber direction, transverse to the fiber direction and off axis tests are commonly used to obtain material behavior at the lamina level. These tests supply a complete response (stress-strain) curve (usually non-linear) with valuable information beyond the proportional limit. The present theory (EST) is based on input that uses only these measured and available test data in conjunction with the laminate stacking sequence and geometry of the problem configuration. Thus, the EST introduced here uses readily available fundamental experimental input leading to a method that can find wide ranging utility, well beyond the example problem addressed herein.

The methodology introduced can also be used to predict damage growth in a general laminate. The laminate is assumed to be built-up as a stack of lamina. Each lamina is modeled as a nonlinear elastic, homogenised, orthotropic layer that can undergo damage. Nonlinear elastic behavior is depicted via three polynomial functions of strain. Two of these functions describe the ratio of secant moduli in fiber and transeverse directions with the initial values of the respective moduli, without damage. The third function describes the behavior of poisson's ratio. Damage is incorporated via three *internal state variables (ISV)*. These ISV's represent the 'thermodynamic forces' to change the state of a material system. Evolution laws of these ISV's incorporate work considerations and thermodynamic requirements, such as, increase in entropy.

2 Theoretical Development

2.1 Non-linear Constitutive Formulation

Schapery [3] developed nonlinear elastic consitutive relations using a work potential approach which accounted for the effect of microdamage. The equations are,

$$\begin{aligned} \sigma_1 &= Q_{11} f_1 \epsilon_1 + Q_{12} f_{12} I_2 \\ \sigma_2 &= Q_{12} f_2 I_1 + Q_{22} f_2 \epsilon_2 \\ \tau_{12} &= Q_{66} \gamma_{12} \end{aligned} \tag{1}$$

where,

$$Q_{11} = \frac{E_{11}}{1 - \nu_{12}\nu_{21}} \quad , \quad Q_{22} = \frac{E_{22}}{1 - \nu_{12}\nu_{21}}$$

$$Q_{12} = \nu_{12} Q_{22} \quad , \quad Q_{66} = G_{12}$$

$$\nu_{21} = \frac{\nu_{12} E_{22}}{E_{11}}$$

The functions, f_1, f_2 and f_{12}, introduce nonlinearity into the constitutive relations. They are defined as,

$$f_{12} \equiv -\frac{1}{\nu_{12}} \frac{d\epsilon_2}{d\epsilon_1}, \quad , \quad f_2 \equiv \frac{E^{90}(\epsilon_2)}{E_{22_0}}$$

$$f_1 \equiv \frac{E^0(\epsilon_1)}{E_{11}}$$

Function f_1, expresses the ratio between the fiber direction secant modulus (E^0) with its initial value (E_{11}). This information is available from a coupon level tensile or compressive test in the fiber direction upto the point of first failure. First failure is associated with fiber kinking (compression) and fiber fracture (tension). Similarly, function f_2 expresses the same in the transverse direction(E^{90} vs E_{22_0}). Function f_{12} expresses the evolution of poisson's ratio, ν_{12}. This can also be characterized using uniaxial tensile loading in fiber direction. f_1 and f_{12} are functions of ϵ_1 and f_2 is a function of ϵ_2.

Integrals I_j appearing in (1) are defined as,

$$I_1 \equiv \int_0^{\epsilon_1} f_{12} d\epsilon_1, \qquad I_2 \equiv \int_0^{\epsilon_2} f_2 d\epsilon_2$$

These definitions of I_j satisfy the reciprocity condition,

$$\frac{\partial \sigma_1}{\partial \epsilon_2} = \frac{\partial \sigma_2}{\partial \epsilon_1}$$

2.2 Damage Modeling through Internal State Variables

In the existing literature on damage mechanics as applied to fiber composite materials, the effect of damage is incorporated through the change

in transverse young's modulus E_{22} and inplane shear modulus G_{12}. For instance, Sun and Chen [4] proposed a one parameter plastic potential in conjunction with orthotropic incremental plasticity theory to study the evolution of E_{22} and G_{12} in tension. Schapery and Sicking [2], used ST to study the evolution of E_{22} and G_{12}. These previous studies were not concerened with the state of the lamina beyond first failure in the fiber direction. Yet, it is recognized [5] that such damage is dominant for compression loaded composite structures. Lamina level coupon tests have shown that fiber direction modulus, E_{11} and poisson's ratio, ν_{12} can be assumed to be independent of microdamage that influence E_{22} and G_{12}. When the fiber direction strain exceeds the fiber kinking strain, then the post kinking response assumes that depicted in figure 2. In tension, fiber fracture occurs and the resulting response is as indicated in figure 3

2.2.1 Elements of Schapery Theory (ST)

In ref [2], *Internal State Variables* are used to incorporate *inelastic* behavior in the material response. Earlier, Schapery [6], introduced a more general thermodynamic framework to study materials that undergo damage. In these developments, the total work done in a mechanical process is assumed to be composed of the inelastic work(W_s) and the work of deformation (W).

$$W_T = W + W_s \tag{2}$$

The irrecoverable portion of total energy (W_s) can be determined from the material stress-strain response as shown in figure 1. Internal state variables or ISV's are described through S_i's. Each S_i is associated with a particular damage mechanism. To satisfy the path independence of total work, these ISV's have to satisfy the following relation,

$$f_i = \frac{\partial W_s}{\partial S_i} \tag{3}$$

Left hand side of equation 3 is called the *thermodynamic force* related to the i^{th} ISV. An estimate of the available thermodynamic force could be obtained from the relation,

$$f_i \equiv -\frac{\partial W}{\partial S_i} \tag{4}$$

Schapery considered two ISV's. They were the energies associated with matrix microcracks (S) and of the transverse intra-ply cracks (S_c), respectively. Inelastic work is described as ,

$$W_s = S + S_c \tag{5}$$

These ISV's are related to E_{22} and G_{12} through (6)

$$\begin{aligned} E_{22} &= E_{22_0} e_s(S) e_c(S_c) \\ G_{12} &= G_{12_0} g_s(S) g_c(S_c) \end{aligned} \tag{6}$$

Here, E_{22_0} and G_{12_0} are transverse and shear moduli of the virgin material, ie, at zero strain and zero damage; $e_s(S)$ and $g_s(S)$ are factors relating these two moduli to microdamage ISV, S and $e_c(S_c)$ and $g_c(S_c)$ are factors relating E_{22} and G_{12} to the transverse cracking ISV, S_c.

The functions e_s, e_c, g_s and g_c are expressed as polynomial relations in respective ISV's ([2]). Assuming that the thermal expansion or contraction strains are independent of damage, we obtain the following form for the strain energy density (or work of deformation) W.

$$W = Q_{11} I_{11} + Q_{22} I_{22} + \nu_{12} Q_{22} I_1 I_2 + \frac{G_{12} \gamma_{12}^2}{2} \tag{7}$$

where,

$$I_{11} \equiv \int_0^{\epsilon_1} \epsilon_1 f_1 d\epsilon_1 \qquad I_{22} \equiv \int_0^{\epsilon_2} \epsilon_2 f_2 d\epsilon_2$$

To incorporate geometric nonlinearities, Greens' strains and the second Piola Kirchoff stresses need to be used in the expression for W. For small strains, (7) would contain only the first order terms in the strain-displacement relations.

Using equations (3)-(7), we obtain,

$$I_{11} \frac{\partial Q_{11}}{\partial S} + (I_{22} + \nu_{12} I_1 I_2) \frac{\partial Q_{22}}{\partial S} + \frac{\gamma_{12}^2}{2} \frac{\partial G_{12}}{\partial S} = -1$$

$$I_{11}\frac{\partial Q_{11}}{\partial S_c} + (I_{22} + \nu_{12} I_1 I_2)\frac{\partial Q_{22}}{\partial S_c} + \frac{\gamma_{12}^2}{2}\frac{\partial G_{12}}{\partial S_c} = -1$$

Since the fiber direction stiffnesses are unaffected by S and S_c, the first terms in these equations can be neglected. Also, $\nu_{12}\nu_{21} \ll 1$. Thus the above equations reduce to,

$$(I_{22} + \nu_{12} I_1 I_2)\frac{\partial E_{22}}{\partial S} + \frac{\gamma_{12}^2}{2}\frac{\partial G_{12}}{\partial S} = -1$$
$$(I_{22} + \nu_{12} I_1 I_2)\frac{\partial E_{22}}{\partial S_c} + \frac{\gamma_{12}^2}{2}\frac{\partial G_{12}}{\partial S_c} = -1$$

For an inelastic process the entropy production rate is non-negative. Hence,

$$\dot{S} + \dot{S}_c \geq 0$$

The overdots represent temporal derivatives. Physically, $\dot{S}$ and $\dot{S}_c$ are both non-negative because healing (or reversible damage) is not allowed. Thus $\dot{S} + \dot{S}_c \geq 0$ is strictly enforced.

From experiments ([2]), it has been observed that for small strains, S behaves as ϵ^3. Thus to express the moduli, E_{22} and G_{12} in terms of a polynomial of S, a reduced variable S_r can be used,

$$S_r \equiv S^{1/3} \tag{8}$$

The equation to determine S_r now becomes,

$$(I_{22} + \nu_{12} I_1 I_2)\frac{\partial E_{22}}{\partial S_r} + \frac{\gamma_{12}^2}{2}\frac{\partial G_{12}}{\partial S_r} = -3S_r^2 \tag{9}$$

The effect of transverse inter-ply cracking is not as easily measurable as the effect of microdamage due to matrix microcracking. An estimate can be obtained using equation 9 to approximate S_r and then using the following relation,

$$S_c = W_T - W - S \tag{10}$$

In the present study, we assume that matrix microcracking is the only responsible mechanism for transverse property degradation. A detailed discussion of obtaining S_c is provided in ref [2].

2.3 Fiber Direction Damage - Extended Schapery Theory (EST)

The theory presented upto now is for a continuous evolution of the strain functions, f_1, f_2 and f_{12}. In its present form it is inadequate to incorporate post-kinking response (compression) or post-fracture response (tension). The salient features of the fiber direction response are shown in figures 2 and 3.

A new ISV associated with fiber direction damage is introduced to incorporate response beyond kinking (compression) and fiber fracture (tension). It has been observed in laboratory tests that a material behaves differently for tensile and compressive loading along the fiber direction. While, local fiber microbuckling/kinking due to the presence of local imperfections is the main mode of failure in compression([7],[8],[9], [10]), tensile failure is due to fiber fracture, appearing as cracks perpendicular to the loading direction.

The tensile response shows a clear loss of stiffness at failure and the residual strength goes to zero immediately after failure. The compressive response shows the presence of residual strength after failure giving an impression of transforming into a different new material. We note that Rajagopal et al, [11] have established a general thermodynamic framework to address material microstructure evolution in finite strain setting.

With a new ISV introduced, equation 5 becomes,

$$W_s = S_w + S + S_c \tag{11}$$

The ISV S_w represents the inelastic behavior in the fiber direction due to compressive kinking or fiber fracture. Hence, S_w is not present in the initial elastic regime. It can be computed from the material stress-strain curve under compressive loading in fiber direction (figure **??**. Once kinking or fiber fracture occurs, S_w takes a finite jump. The finite jump in S_w in compression is termed the kinking toughness and is a material property that is unique to a fiber reinforced lamina and is a measurable quantity. S_w is related to the fiber direction secant modulus, E_{11} via relations similar to the moduli in other directions.

$$E_{11} = E_{11_0} h(S_w) \tag{12}$$

Using equations (11, 3 and 4) we can obtain S_w at every state of strain as,

$$I_{11} \frac{\partial Q_{11}}{\partial S_w} = -1 \tag{13}$$

3 Application of EST

3.1 Plate with a hole

The EST introduced in the previous section was implemented in the commercially available finite element package ABAQUS, and results were obtained for a unidirectional notched plate with a central circular hole under compressive loading. The analysis incorporated geometric nonlinearity. Due to symmetry, only a quarter of the plate is analysed. The problem geometry is shown in figure 6. The plate was stressed until the damage zone initiating at the edge of the notch reached the boundary of the plate simulating a test program in which the plate is stressed to complete failure.

3.2 Modeling in ABAQUS

3.2.1 Geometry

The geometry depicted in figure 6 was meshed using plane stress 2-D continum elements, CPS4. End loading was provided by specifying displacement boundary conditions at the edge of the plate. Symmetric boundary conditions were enforced on the two sides adjacent to the hole.

3.2.2 Material Model

In the commercially available FE code ABAQUS, it is possible to introduce user defined material behavior through user written subroutines. To that end, the user need to provide the incremental stress-strain relationships or the material jacobian (J) and update the stress and /or any internal state variables to their values at the end of each increment. This user subroutine would be called by ABAQUS at every material point, where the user defined material is included.

The material data for the present study was obtained from [5]. The material is modeled as homogenised orthotropic nonlinear elastic material obeying EST. With a view to extending the present work to model stringer stiffened notched panels in compression ([5]), we were interested in obtainingthe complete material response curves for AS4/3501-6. Hence the data given in [2] for AS4/3502 was used to approximate the relevant functional parameters f_1, f_2, f_{12}, $e_s(S_r)$ and $g_s(S_r)$. Available parameters were scaled down by the ratio of moduli of AS4/3501-6 and AS4/3502. A typical coefficient A_{ij} was modified as,

$$A_{ij}^{3501} = A_{ij}^{3502} \frac{E^{3501}}{E^{3502}}$$

The modified set of parameters for the 0-layer are given in table 2.

As stated earlier, in the present work only S_w and S_r are used as damage parameters since the mechanisms of damage that are considered are matrix microcracking and fiber direction damage.

4 Results

Two meshes (figures 7 and 8) with different mesh densities were used to generate the finite element results. From the results, we obtain the variation of reaction force against the applied end shortening. We also plot the fraction of undamaged material remaining in the system against applied end shortening. Figures are provided to show the growth of damage through different loading positions for the finer mesh.

5 Discussion

Initially the response of the plate is elastic. Therefore the reaction force against the applied end shortening ($P-\Delta$) curve is linear (slight elastic nonlinearity is incorporated through the f_{ij}'s, however,

this does not show a visible effect on the $P-\Delta$ curve)- see figure 10. When the material elements adjacent to the hole reaches a critical strain corresponding to fiber kinking a damage zone is found to initiate at the edge of the hole. This is depicted in figure 13 where we show the progression of damage as darkened elements on the finite element grid (this is shown only for the finer mesh, however, the salient features of the damage progression were very similar for the coarser mesh as well). The corresponding $P-\Delta$ curve shows softening due to the kink band formation and propagation away from the edge of the hole. In figure 9 we show results for both meshes. Clearly the $P-\Delta$ curve does not show an appreciable change between the meshes, lending confidence to the choice of the finer mesh. In figures 11 and 12, we have plotted the area fraction corresponding to undamaged material against the applied end-shortening. As is evident, as damage progresses, the rate at which the kink band engulfs more and more material, increases. We note that the present results are remarkably in good agreement with previous experimental results ([12]), on uniply model composite plates with a circular hole, where it was observed that fiber kink banding initiated and propagated in the manner that has been simulated in the present work.

We also studied the effect of the plateau stress magnitude on the residual strength. We did this by lowering the plateau stress to 25% of the kinking stress (case 2) (earlier, the plateau stress was 50% of the kinking stress (case 1))- see figure 5. The $P-\Delta$ curve, corresponding to this latter case, is shown in figure 10 where we have also shown the $P-\Delta$ curve corresponding to the earlier (plateau stress= 50% of the kinking stress) results. The lowering of the plateau stress leads to a drastic reduction (almost 50%) in the maximum load carrying capability of the notched panel. Thus, both the kinking stress and the plateau stress are important material properties associated with the compressive characterization of a fiber reinforced lamina. In fact, as discussed earlier, the area under the fiber direction compressive stress-strain curve upto the point of the initiation of the plateau stress is termed the kinking toughness and this parameter is an experimentally measuarable quantity. Alternatively, micromechanics modeling can be used ([9]) to extract the kinking toughness from the fiber and matrix non-linear properties and the fiber volume fraction. Extension of the present methodology to analyse the experimental data on stringer reinforced stiffened compressively loaded notched panels ([5]) is presently being carried out and results will be reported in the near future.

6 Conclusion

A non-linear elastic/damage methodology has been presented and numerically implemented to study progressive failure in fiber reinforced composite materials. The usefulness of the present methodology has been demonstrated by examining the compressive response of a unidirectional notched composite plate. The numerical results capture the experimental observations that have been reported before in the open literature. The present work has succesfully addressed the important problem of modeling unstable local material response (fiber kinking) in a global setting, where the structure is still stable. That is, we have provided a macroscopic methodology to analyze compressively loaded composite structures in the presence of locally unstable material response. The usefulness of knowing the compressive kinking toughness of a fiber reinforced lamina (measured experimentaly or modeled and extracted using micromechanics) has been demonstrated. The utility of the present work is far reaching in the analysis and design of damage tolerant composite structures.

References

[1] Fu-Kuo Chang and K.Y. Chang. A Progressive Damage Model for Laminated Composites Containing Stress Concentrations. *Journal of Composite Materials*, 21:834–855, September 1987.

[2] R.A. Schapery and D.L. Sicking. On Nonlinear Constitutive Equations for Elastic and Viscoelastic Composites with Growing Damage. *Mechanical Behavior of Materials*, 47:45–76, June 1995.

[3] R.A. Schapery. Mechanical Characterization and Analysis of Inelastic Composite Laminates with Growing Damage. *Mechanics of Composite Materials and Structures*, AMD-100:1–9, June 1989.

[4] C.T.Sun and J.L.Chen. A Simple Flow Rule for Characterizing Nonlinear Behavior of Fiber Composites. *Journal of Composite Materials*, 23:1009–1020, October 1989.

[5] Carlos G.Dávila, Damodar R. Ambur, and David M. McGowan. Analytical Prediction of Damage Growth in Notched Composite Panels Loaded in Compression. *Journal of Aircraft*, 37(5):898–905, September–October 2000.

[6] R.A. Schapery. A Theory of Mechanical Behavior of Elastic Media with Growing Damage and other Changes in Structure. *J. Mech. Phys. Solids*, 38(2):215–253, June 1990.

[7] C R Schultheisz and A M Waas. Compressive Failure of Composites 1. Testing and Micromechanical Theories. *PROG. AEROSP SCI*, 32(1):1–42, 1996.

[8] A M Waas and C R Schultheisz. Compressive Failure of Composites 2. Experimental Studies. *PROG. AEROSP SCI*, 32(1):43–78, 1996.

[9] J. H. Ahn and Anthony M. Waas. Prediction of Compressive Failure in Laminated Composites at Room and Elevated Temperature. *AIAA Journal*, 40(2):2002, February 2002.

[10] Chandra S. Yerramalli and Anthony M. Waas. Compressive Splitting Failure of Composites using Modified Shear Lag Theory. *International Journal of Fracture*, pages 1–14, 2002.

[11] K. Rajagopal and A. Wineman. On a Constitutive Theory for Materials undergoing Microstructural Changes. *Archives of Mechanics*, 42:53–57, July 1990.

[12] Amir Reza Khamseh and Anthony M. Waas. Failure of Uniply Model Composites under Compression. *ASME Trans. J. of Eng. Materials and Technology*, 114:304–310, July 1992.

7 Appendix

	AS4/3501-6
Moduli	
E_L, Msi	15.30
E_T, Msi	1.60
G_{LT}, Msi	0.8
ν_{12}	0.34

Table 1: Material Constants

Exponent	f_1	f_2(comp)	f_2(tens)	f_{12}
0	1	1	1	1
1	4.429	5.5220	-5.5220	-14.6
2	-29.5346	-43.145	-27.9337	-594.8290

Table 2: Coefficients used in numerical modeling

	End Displacement (in)
A	0.020
B	0.025
C	0.030
D	0.035
E	0.037
F	0.038

Table 3: Loading stages where kind band progression is shown in figure 13

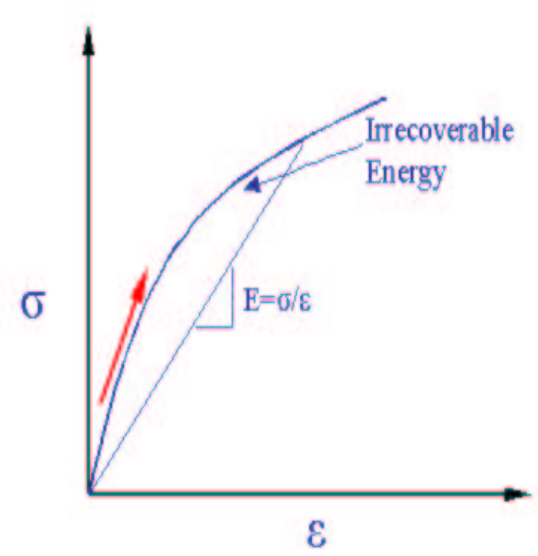

Figure 1: Determination of irrecoverable energy from stress-strain response

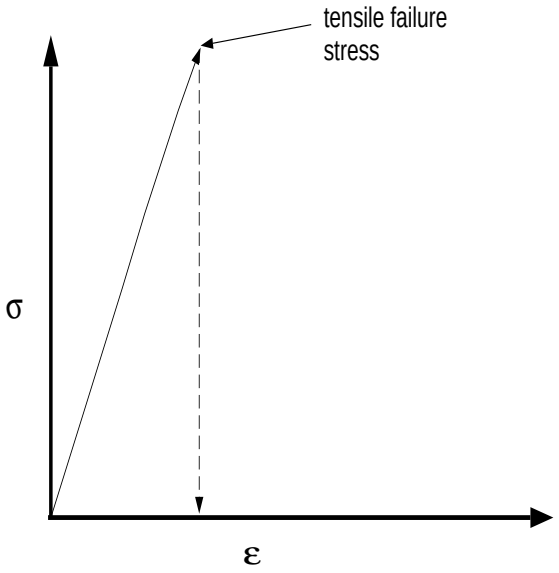

Figure 3: Typical tensile stress-strain behavior

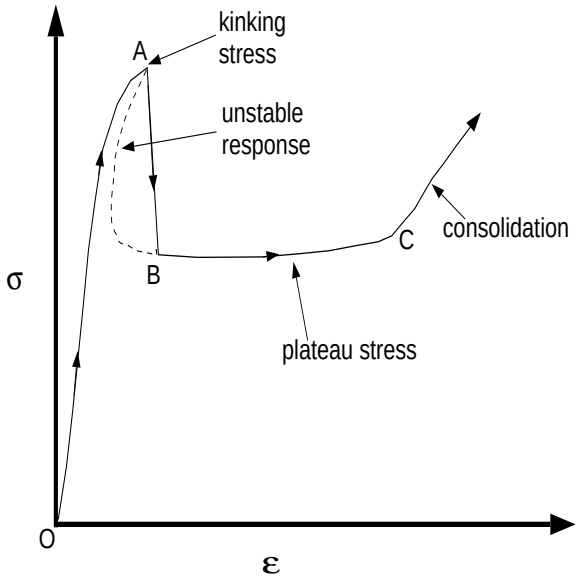

Figure 2: Typical compressive stress-strain behavior

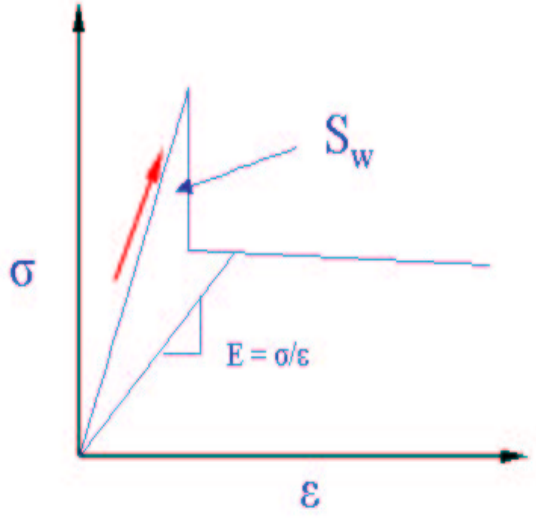

Figure 4: Determination of S_w from stress-strain response

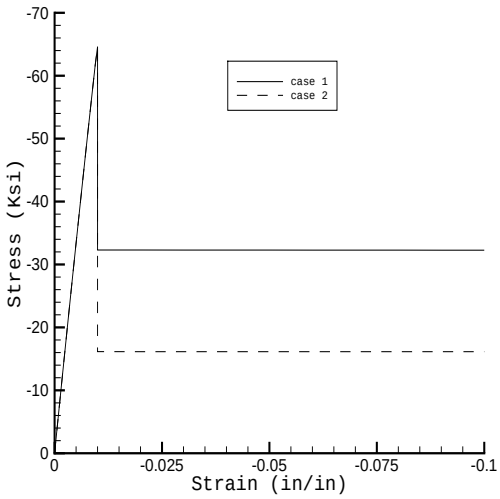

Figure 5: Stress-strain curves input to ABAQUS

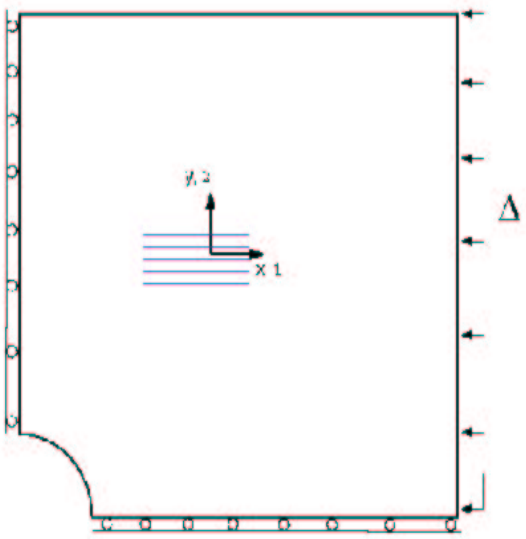

Figure 6: Geometry of the plate with a hole (fiber direction is parallel to x-direction)

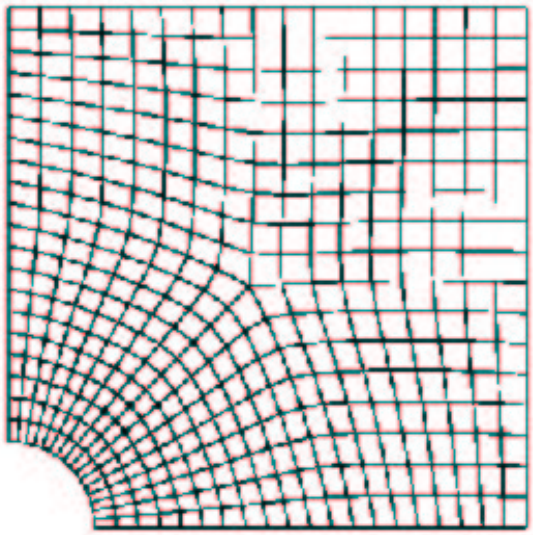

Figure 7: Coarser mesh (mesh A)

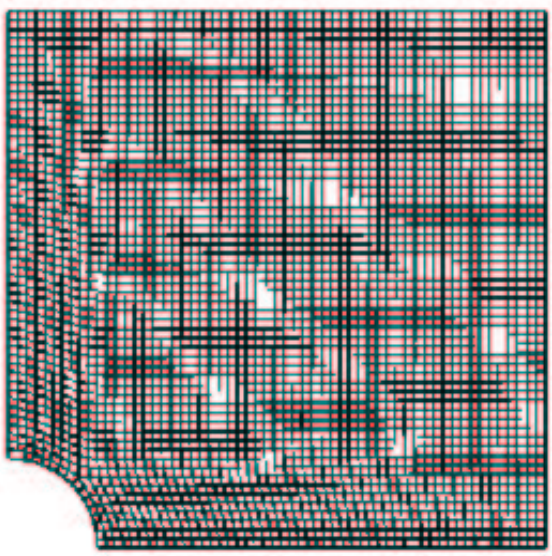

Figure 8: Finer mesh (mesh B)

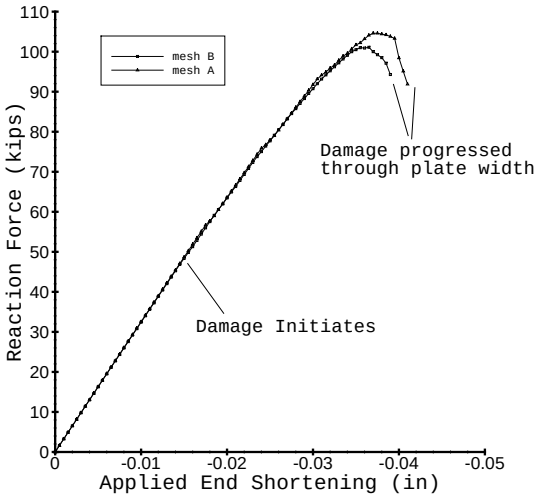

Figure 9: Global Reaction Force against End Shortening for meshes 1 and 2

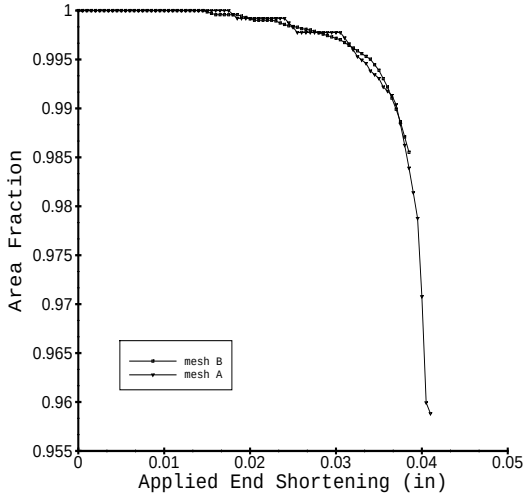

Figure 11: Lowering of undamaged area fraction with end displacement for meshes A and B

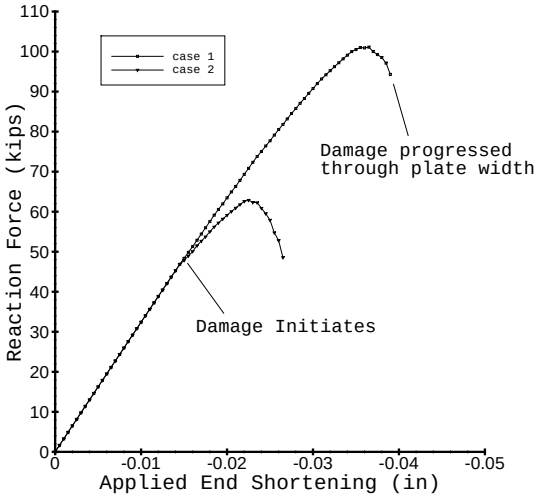

Figure 10: Global Reaction Force against End Shortening for cases 1 and 2

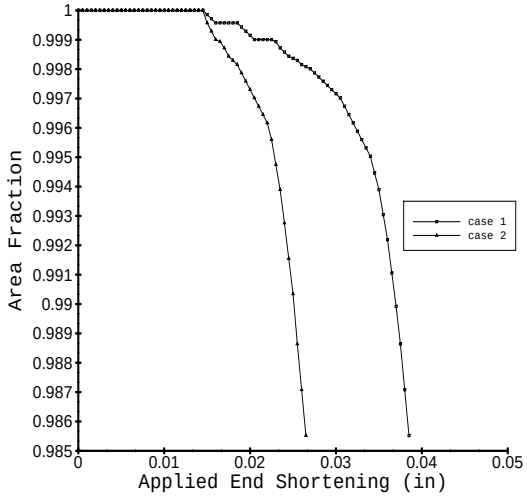

Figure 12: Lowering of undamaged area fraction with end displacement for cases 1 and 2

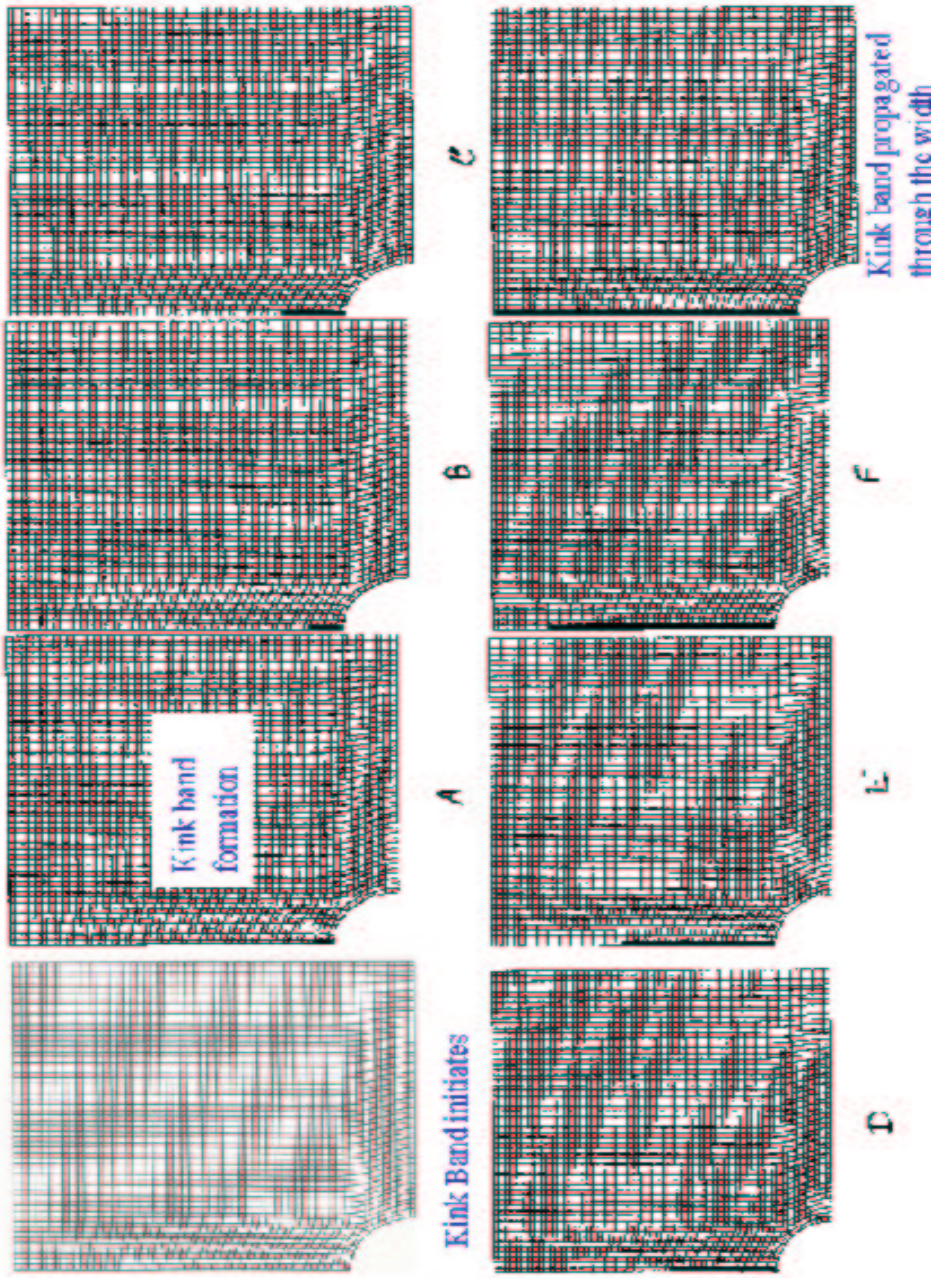

Figure 13: Initiation and progression of kink band with end displacement case 1 and mesh B (for explanation of A,B,C, etc, see table 3)